

A Finite State Aerodynamic Model for a Lifting Surface in Incompressible Flow

Yoshikazu Miyazawa*

National Aerospace Laboratory, Tokyo, Japan

and

Kyuichiro Washizu†

Osaka University, Osaka, Japan

An aerodynamic model necessary for a state equation of an aeroelastic system is proposed. The system is assumed to be a lifting surface in incompressible flow. The model consists of a nonmemory component and a memory component. The former is directly expressed by generalized coordinates. The latter is approximately expressed by using augmented system which is strictly proper and of finite dimension. The augmented system is constructed from Marcov parameters which are derived from an appropriate numerical computation of unsteady aerodynamics. A simple example is given to illustrate the approximation properties of the model. The characteristics of the model are: 1) no complex parameters are necessary to determine the model, 2) system stability of the model is easily guaranteed, and 3) accuracy of the model is good in both the high- and low-frequency regions.

Nomenclature

| | |
|---------------------------------|--|
| A_2, A_1, A_0 | = coefficient matrices of the nonmemory component in unsteady aerodynamics |
| $A(k)$ | = aerodynamic matrix in the frequency domain |
| b | = reference semichord [length] |
| $\Delta C_p(x, y, t)$ | = pressure difference between upper and lower surfaces of the wing, dimensionless with respect to $\frac{1}{2}\rho V^2$ |
| $\Delta C_{p_j}^\circ(x, y, t)$ | = impulse response of nondimensional pressure difference produced by the third-order derivative of the j th mode input |
| f | = generalized force, dimensionless with respect to $\frac{1}{2}\rho V^2 b^2$ |
| F, G, H | = triplet of an augmented system |
| g, h | = column vectors in matrices G^T and H |
| I_N | = identity matrix of $R^{N \times N}$ |
| j | = $\sqrt{-1}$ |
| k | = reduced frequency, $\omega b/V$ |
| k_i | = nondimensional natural frequency of the i th mode, $\omega_i b/V$ |
| ℓ | = sequence of discrete time steps |
| m | = number of generalized coordinates |
| m_i | = generalized mass of the i th mode |
| N | = order of an augmented system |
| p | = degree of approximation |
| q | = generalized coordinate |
| $R^m, R^{N \times N}$ | = sets of real vector and matrix |
| S_0, S_1 | = Hankel matrices defined by Eq. (18) |
| t, τ | = time, dimensionless with respect to b/V |
| V | = freestream velocity [length/time] |
| w | = downwash distribution on the wing, dimensionless with respect to V |
| x, y, ξ, η | = space coordinates fixed to the nominal condition of a wing, dimensionless with respect to b |
| $Z_a(x, y, t)$ | = elastic deformation of a wing along Z axis, dimensionless with respect to b |
| $Z_{a_i}(x, y)$ | = i th mode shape, dimensionless with respect to b |

| | |
|--------------------------|---|
| $z(t)$ | = augmented state |
| γ | = intensity of a vortex, dimensionless with respect to bV |
| λ | = characteristic root of an augmented system |
| $\mu(x, y)$ | = mass distribution of a wing, dimensionless with respect to (reference mass)/ b^2 |
| ν | = mass ratio, $\frac{1}{2}\rho b^3/(\text{reference mass})$ |
| ρ | = air density [mass/length ³] |
| $\Phi_{ij}^\circ(t)$ | = impulse response of the i th generalized force due to \ddot{q}_j |
| $\Phi(t)$ | = weighting pattern function of the memory component in unsteady aerodynamics, $\Phi_{ij}(t) = \ddot{\Phi}_{ij}^\circ(t)$ |
| $\Delta\phi(x, y, t)$ | = potential discontinuity on the xy plane, dimensionless with respect to bV |
| ω | = circular frequency [radian/time] |
| ω_i | = natural frequency of the i th vibrational mode [radian/time] |
| $()^T$ | = transpose of the matrix |
| $()^{-1}$ | = inverse of the matrix |
| $\text{diag}\{ \dots \}$ | = diagonal matrix |
| $(), ()'$ | = $d()/dt, \partial()/\partial t$, respectively |
| $()$ | = complex amplitude |
| $()$ | = Fourier transform |

All quantities are dimensionless except as indicated by brackets.

Introduction

RECENT developments of automatic control technology have had a great effect on aircraft design. Various control systems, called active controls technology (ACT), have been proposed to improve aircraft performance. Among them, a flutter control systems is considered to be promising, because flutter can be well damped by modifying aerodynamic forces with appropriate actuation of properly located control surfaces.

There are two distinct approaches in the analysis and synthesis of aeroelastic control systems such as the flutter suppression system: i.e., a frequency domain approach and a state equation approach. Although the state equation approach can be considered to be more useful than the frequency domain approach in the design of control system,¹⁻⁴ it needs finite dimensionalization for the aerodynamics as well as the structural dynamics. In the case of structural dynamics, an expansion method with natural vibrational modes has been established, but regarding the aerodynamics various techniques have only been suggested.

Received Aug. 25, 1981; revision received April 27, 1982. Copyright © American Institute of Aeronautics and Astronautics, Inc., 1982. All rights reserved.

*Research Scientist, Flight Research Division.

†Professor, Department of Mechanical Engineering. Professor Emeritus of the University of Tokyo. Fellow AIAA.

Vepa⁵ originally investigated this problem and suggested a Padé approximant which is a single input and single output rational transfer function fitted to each element of an aerodynamic matrix that is a frequency response of the aerodynamic system. Edwards^{1,6} introduced a generalized unsteady aerodynamic theory for aerodynamic system modeling and suggested a rational model. Since unsteady aerodynamics of a lifting surface are not analytically obtainable, and general numerical calculations are based on simple harmonic analysis,^{7,8} most of the subsequent approximate models are fitted on frequency responses.^{9,10}

The model transfer function, however, often becomes nonanalytic in the right half of the s plane. This means that the open loop aerodynamic system of the model is unstable, although the physical aerodynamic system is stable by itself. The main reasons why the model erroneously becomes unstable are considered to be as follows: 1) the curve fit is highly weighted in the low-frequency region, 2) the simultaneous approximation of nonmemory component and memory component coefficients, and 3) numerical errors in the given aerodynamic data.

To avoid this difficulty, attempts are typically made in which the characteristic roots of the model intuitively are chosen in advance and the remaining coefficients are determined to fit the model to the given frequency response data.¹¹ With this method, not only the frequency points and weighting parameters but also characteristic roots of the model depend on the designer's choice.

A model construction method which overcomes these defects to some extent is proposed in this paper. At first, the dynamics of the total aeroelastic system are exactly described by a differential-integral equation, i.e., time domain analysis is utilized so as to interpret the aerodynamic system, which has to be approximately included in the state equation of the aeroelastic system. As a result, it is noticed that the unsteady aerodynamic forces can be separated into two components—a nonmemory component and a memory component. Since the nonmemory component is expressed directly by generalized coordinates and their derivatives, it does not introduce any difficulty in construction of the state equation. On the other hand, as the memory component is described by a convolution integral of generalized coordinates, it must be approximated by using some appropriate finite dimensional system, which could be called an "augmented system." It is proposed here that the augmented system could be constructed by partial realization of Marcov parameters of the exact aerodynamic system. The degree of the partial realization is the only variable which the designer must choose in advance. In order to compare this aerodynamic model with preceding models, it is interpreted in the frequency domain.

A simple numerical example is given to illustrate this approach. Marcov parameters necessary for the modeling are obtained from discrete-time responses calculated by a vortex lattice method. Accuracy of the model is evaluated in the frequency domain. The frequency responses of the model are compared with those obtained by numerical computations of simple harmonic analysis at discrete frequency points. The difference is small and the system stability of the model is also guaranteed.

Equation of Motion and Unsteady Aerodynamics

Dynamic motion of a flexible structure excited by some external forces is generally approximated by linear ordinary differential equations of finite number. The linearization is introduced by supposing that deviation from a nominal condition is small. The finite dimensionalization is carried out by assuming that the deviation can be approximated with modes of finite number. It is known empirically that the expansion with a number of characteristic modes is sufficient to simulate aeroelastic phenomena such as aircraft flutter.

For simplicity in this paper, a flexible wing as shown in Fig. 1 is considered. Coordinate axes are fixed on the nominal

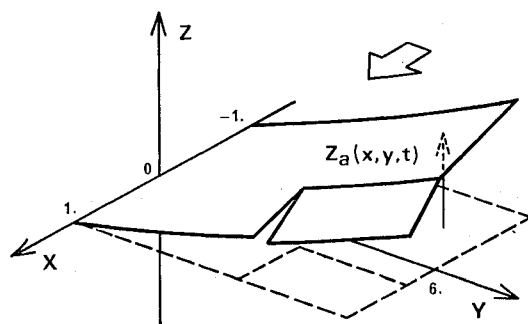


Fig. 1 Lifting surface in incompressible flow.

condition of the flexible wing moving with constant speed V . Small deviation along the Z axis, $Z_a(x, y, t)$, is expanded by m modes.

$$Z_a(x, y, t) = \sum_{i=1}^m Z_{a_i}(x, y) q_i(t) \quad (1)$$

where $Z_{a_i}(x, y)$ and $q_i(t)$ are the i th mode shape and a corresponding generalized coordinate, respectively. In this paper all quantities are nondimensional except as indicated in Nomenclature. Suppose $Z_{a_i}(x, y)$ are characteristic modes; the lifting surface can then be expressed by the following decoupled dynamic equation of motion.

$$m_i \ddot{q}_i(t) + m_i k_i^2 q_i(t) = v f_i(t) \quad \text{for } i = 1, \dots, m \quad (2)$$

Time t is dimensionless with respect to reference time b/V ; therefore, the time derivative has a relation $(\dot{}) = (b/V) d()/dt^*$ where t^* is a dimensional time. m_i is a generalized mass which is defined with nondimensional mass distribution of the wing $\mu(x, y)$.

$$m_i = \iint_{\text{wing}} \mu(x, y) Z_{a_i}^2(x, y) dx dy \quad (3)$$

where $\iint_{\text{wing}} dx dy$ is the integral over the region of the wing. $f_i(t)$ is a generalized aerodynamic force acting on the i th mode, which can be defined by the pressure difference distribution.

$$f_i(t) = \iint_{\text{wing}} \Delta C_p(x, y, t) Z_{a_i}(x, y) dx dy \quad (4)$$

There are two types of aerodynamic forces, i.e., the external aerodynamic force produced by gusts and the self-excited aerodynamic force induced by the deviation and motion of the wing itself. Since the former does not have an effect on the system stability and damping, only the latter aerodynamic force is investigated. Furthermore, the flowfield is assumed to be incompressible.

The aerodynamic force is linearized by assuming that the deviation of the wing is small, as in the case of structural dynamics modeling. The relation between downwash w and pressure distribution of a lifting surface ΔC_p is expressed as follows:

$$w(x, y, t) = - \frac{1}{8\pi} \int_0^\infty \iint_{\text{wing}} \frac{\Delta C_p(\xi, \eta, t-\tau) d\xi d\eta d\tau}{[(x-\xi-\tau)^2 + (y-\eta)^2]^{3/2}} \quad (5)$$

where w is dimensionless with respect to freestream velocity V and the symbol \iint means that the integral is defined in the finite part sense.

From Eq. (1), downwash distribution is written as

$$w(x, y, t) = \sum_{i=1}^m \left\{ \frac{\partial Z_{a_i}(x, y)}{\partial x} q_i(t) + Z_{a_i}(x, y) \dot{q}_i(t) \right\} \quad (6)$$

In order to construct a state equation of the total aeroelastic system, the generalized aerodynamic forces must be expressed explicitly by the generalized coordinates. The explicit form of the aerodynamic forces can be formulated by considering an impulse response of pressure distribution produced by an input of the third-order derivative of each generalized coordinate $\ddot{q}_j(t)$; that is,

$$q_j(t) = 0; t < 0, \quad q_j(t) = t^2/2; t \geq 0 \quad (7)$$

The response of pressure distribution with this input is defined as $\Delta C_{p_j}^\circ(x, y, t)$. The specific input (7) is given so that the response $\Delta C_{p_j}^\circ(x, y, t)$ can be a finite value excluding the points where the downwash distribution is not continuous.

The pressure distribution produced by an arbitrary motion of the j th mode, $\Delta C_{p_j}(x, y, t)$, is written by the following convolution integral.

$$\Delta C_{p_j}(x, y, t) = \int_{-\infty}^t \Delta C_{p_j}^\circ(x, y, t-\tau) \ddot{q}_j(\tau) d\tau \quad (8)$$

The equation can be transformed by partial integration.

$$\begin{aligned} \Delta C_{p_j}(x, y, t) &= \Delta C_{p_j}^\circ(x, y, 0) \ddot{q}_j(t) + \Delta C_{p_j}^{\circ'}(x, y, 0+) \dot{q}_j(t) \\ &+ \Delta C_{p_j}^{\circ''}(x, y, 0+) q_j(t) + \int_{-\infty}^t \Delta C_{p_j}^{\circ'''}(x, y, t-\tau) q_j(\tau) d\tau \end{aligned} \quad (9)$$

where () and ()' denote $d()/dt$ and $\partial()/\partial t$, respectively.

The impulse response of the i th generalized aerodynamic force due to $\ddot{q}_j(t)$ is defined as $\Phi_{ij}^\circ(t)$, namely,

$$\Phi_{ij}^\circ(t) = \int \int_{\text{wing}} \Delta C_{p_j}^\circ(x, y, t) Z_{a_i}(x, y) dx dy \quad (10)$$

The i th generalized aerodynamic force produced by an arbitrary motion of the j th generalized coordinate, $f_{ij}(t)$, can be introduced in the same way as the pressure response.

$$\begin{aligned} f_{ij}(t) &= A_{2ij} \ddot{q}_j(t) + A_{1ij} \dot{q}_j(t) + A_{0ij} q_j(t) \\ &+ \int_{-\infty}^t \Phi_{ij}(t-\tau) q_j(\tau) d\tau \end{aligned} \quad (11)$$

where

$$\begin{aligned} A_{2ij} &= \Phi_{ij}^\circ(0) = \int \int_{\text{wing}} \Delta C_{p_j}^\circ(x, y, 0) Z_{a_i}(x, y) dx dy \\ A_{1ij} &= \dot{\Phi}_{ij}^\circ(0+) = \int \int_{\text{wing}} \Delta C_{p_j}^{\circ'}(x, y, 0+) Z_{a_i}(x, y) dx dy \\ A_{0ij} &= \ddot{\Phi}_{ij}^\circ(0+) = \int \int_{\text{wing}} \Delta C_{p_j}^{\circ''}(x, y, 0+) Z_{a_i}(x, y) dx dy \\ \Phi_{ij}(t) &= \ddot{\Phi}_{ij}^\circ(t) = \int \int_{\text{wing}} \Delta C_{p_j}^{\circ'''}(x, y, t) Z_{a_i}(x, y) dx dy \end{aligned} \quad (12)$$

Because of system linearity, the generalized aerodynamic forces are expressed by the superposition of the generalized

aerodynamic forces produced by each mode input, and are written in matrix and vector form as follows,

$$f(t) = A_2 \ddot{q}(t) + A_1 \dot{q}(t) + A_0 q(t) + \int_{-\infty}^t \Phi(t-\tau) q(\tau) d\tau \quad (13)$$

where vectors $f, q \in R^m$ consist of the generalized forces and the generalized coordinates, respectively. The elements of matrices $A_2, A_1, A_0, \Phi \in R^{m \times m}$ are defined by Eq. (12). $-A_2$ is known as a virtual mass matrix. Since the steady aerodynamic forces corresponding to each mode are finite, an integral of $\Phi(t)$, i.e., $\int_0^\infty \Phi(t) dt$ is also finite value.

The combination of the equations of motion on structural dynamics (2) and the explicit form of the unsteady aerodynamic forces (13) produces an equation of the total aeroelastic system. Such a differential-integral equation is, however, too complicated to use in practice. The nonmemory component, which consists of the first three terms of Eq. (13), is directly expressed by the generalized coordinates and their derivatives. The memory component, the last term in Eq. (13), is a convolution integral with respect to generalized coordinates of the past time value. The nonmemory component does not introduce any difficulty for state equation construction of the aeroelastic system. On the other hand, the memory component must be approximated by outputs of a strictly proper system of finite dimension, inputs of which are generalized coordinates. The problem of how to construct the augmented system that approximates the memory component in aerodynamic forces, namely finite dimensionalization of unsteady aerodynamics, is discussed in the next section.

Approximate Model of the Aerodynamic System

The general form of an N dimensional, strictly proper system is expressed by the following state equation:

$$\dot{z}(t) = Fz(t) + Gq(t) \quad f_{\text{memo}}(t) = Hz(t) \quad (14)$$

$z \in R^N$ is a state. In this case the input is the generalized coordinate $q \in R^N$ and the output is the memory component in aerodynamic forces $f_{\text{memo}} \in R^N$. Constant matrices $F \in R^{N \times N}$, $G \in R^{N \times m}$, $H \in R^{m \times N}$ are called a triplet of the system. If the memory component is approximated by the augmented system (14), the total aerodynamic force of this approximate model f_{model} is described by

$$\begin{aligned} f_{\text{model}}(t) &= A_2 \ddot{q}(t) + A_1 \dot{q}(t) + A_0 q(t) + Hz(t) \\ \dot{z}(t) &= Fz(t) + Gq(t) \end{aligned} \quad (15)$$

It is a characteristic of this model that the nonmemory component of the aerodynamic force is expressed exactly and the memory component is approximated by the output of the finite dimensional system. If the triplet of the augmented system (F, G, H) is appropriately given, the state equation that approximates the dynamics of the total aeroelastic system can be readily obtained by combining Eqs. (2) and (15). In this state equation, the state consists of \dot{q} , q , and augmented state z .

If the augmented system (14) is exponentially stable, i.e., all characteristic roots are in the left half of the s plane, the input and output relation can be written by the following convolution integral.¹²

$$f_{\text{memo}}(t) = \int_{-\infty}^t \text{Hexp}[F(t-\tau)] Gq(\tau) d\tau \quad (16)$$

$\text{Hexp}[Ft]G$ is a weighting pattern function of the augmented system. System order N and parameters in the triplet (F, G, H) can be arranged to approximate $\Phi(t)$, which is the true

weighting pattern function of the memory component in aerodynamic system.

A simple but reliable method is proposed for the problem of determining the augmented system. The model is constructed by utilizing the consistency of the Maclaurin series of weighting pattern functions of the model and the exact aerodynamic system to some order. Coefficients in the Maclaurin series are called Marcov parameters. The conditions are written as follows:

$$\begin{aligned} HG &= \Phi(0), \quad HFG = \dot{\Phi}(0+), \quad HF^2G = \ddot{\Phi}(0+), \dots, \\ HF^{2p-2}G &= \Phi^{(2p-2)}(0+), \quad HF^{2p-1}G = \Phi^{(2p-1)}(0+) \end{aligned} \quad (17)$$

where the integer $p (\geq 1)$ is an arbitrarily given design parameter which indicates the degree of approximation. Solving Eq. (17), i.e., the minimal partial realization problem, has been discussed in Refs. 13 and 14. Since a model that satisfies the given Marcov parameters can not be determined uniquely in some cases, a general engineering solution to this problem has not yet been established. However, if the following assumption can be guaranteed, a finite state model is easily obtained.

Hankel matrices $S_0, S_1 \in R^{mp \times mp}$, which consist of Marcov parameters, are defined as

$$\begin{aligned} S_0 &= \begin{bmatrix} \Phi(0), & \dot{\Phi}(0+) \dots \Phi^{(p-1)}(0+) \\ \dot{\Phi}(0+), & \ddot{\Phi}(0+) \\ \vdots & \vdots \\ \Phi^{(p-1)}(0+) & \dots \Phi^{(2p-2)}(0+) \end{bmatrix} \\ S_1 &= \begin{bmatrix} \dot{\Phi}(0+), & \ddot{\Phi}(0+) \dots \Phi^{(p)}(0+) \\ \ddot{\Phi}(0+), & \ddot{\Phi}(0+) \\ \vdots & \vdots \\ \Phi^{(p)}(0+) & \dots \Phi^{(2p-1)}(0+) \end{bmatrix} \end{aligned} \quad (18)$$

Assumption: The Hankel matrix S_0 is nonsingular and thus has an inverse matrix.

If the above assumption is satisfied, the weighting pattern function of the augmented system is uniquely determined from conditions (17) and the triplet of the system (F, G, H) is given as

$$F = S_0^{-1} S_1, \quad G = E_m^T, \quad H = E_m S_0 \quad (19)$$

where $E_m \in R^{m \times mp}$ is defined as

$$E_m = [I_m, 0] \quad (20)$$

The input and output relation of a system is consistent under the similarity transformation,¹⁴ i.e., the system $(T^{-1}FT, T^{-1}G, HT)$ gives the same input and output relation as that of the system (F, G, H) , where T is an arbitrary nonsingular matrix, the triplet defined by Eq. (19) is one realization of the augmented system, and hence formulations are possible which give other sets of triplet of the equivalent system.

It can be confirmed that the system triplet (F, G, H) defined by Eq. (19) satisfies condition (17) and that the system is controllable and observable. Controllability and observability are the necessary and sufficient conditions for system minimal realization. Although the assumption certainly narrows the

problem mathematically, it is generally satisfied in aerodynamic force modeling of a lifting surface.[‡]

The interpretation of the model in the frequency domain, which may be more general in aerodynamic force modeling, is conducted to make the characteristics of the model clearer. The relation between the input and output complex amplitude of the aerodynamic system is expressed by the so called aerodynamic matrix $A(k)$.

$$\bar{f} = A(k) \bar{q} \quad (21)$$

where $(\bar{})$ denotes the complex amplitude and k is a reduced frequency of the system.

Since the aerodynamic system is expressed by Eq. (13) in the time domain, its frequency response is described by,

$$\begin{aligned} A(k) &= -k^2 A_2 + (jk) A_1 + A_0 + \bar{\Phi}(k) \\ \bar{\Phi}(k) &= \int_0^\infty \Phi(t) e^{-jkt} dt \end{aligned} \quad (22)$$

This aerodynamic matrix can be expanded with asymptotic series using the weighting pattern function $\Phi(t)$.

$$\begin{aligned} A(k) &= -k^2 A_2 + (jk) A_1 + A_0 + (jk)^{-1} \Phi(0) + (jk)^{-2} \dot{\Phi}(0+) \\ &\quad \dots + (jk)^{-2p} \Phi^{(2p-1)}(0+) + (jk)^{-2p-1} \left\{ \Phi^{(2p)}(0+) \right. \\ &\quad \left. + \int_0^\infty \Phi^{(2p+1)}(t) e^{-jkt} dt \right\} \end{aligned} \quad (23)$$

A_2, A_1, A_0 and Marcov parameters of the memory component, which have been defined in the time domain [Eqs. (12) and (17)], are coefficients of asymptotic series in the frequency response. From Eq. (15) a frequency response of the approximate model, A_{model} is

$$A_{\text{model}}(k) = -k^2 A_2 + (jk) A_1 + A_0 + H(jkI_N - F)^{-1} G \quad (24)$$

It is also expressed by the following asymptotic series,

$$\begin{aligned} A_{\text{model}}(k) &= -k^2 A_2 + (jk) A_1 + A_0 + (jk)^{-1} HG \\ &\quad + (jk)^{-2} HFG \dots + (jk)^{-2p} HF^{2p-1} G + (jk)^{-2p-1} \\ &\quad \times \{ HF^{2p} G + HF^{2p+1} (jkI_N - F)^{-1} G \} \end{aligned} \quad (25)$$

Comparing Eqs. (23) and (25), it is noted that the difference between the exact aerodynamic system and the model is caused by the last terms in each equation. Therefore in the region of large k , the response of the model is consistent with the exact response to the $(-2p)$ th order of jk .

A Model with a Consistency Condition in Static Aerodynamics

Considering the requirement that the model must have sufficient accuracy in the low-frequency region from the practical standpoint, the condition of consistency in steady aerodynamics can be taken into account as follows. From Eq.

[‡]As an exception, the rank of Hankel matrix S_0 may possibly be reduced in a limited case where a high aspect ratio wing has a very similar bending and torsion mode shape in the spanwise direction, changing so slowly that a strip theory is applicable. Even in this case, however, the augmented system can be obtained with a slightly modified numerical algorithm.

(13) a steady aerodynamic force f_{st} produced by a constant input q_{st} is

$$f_{st} = \left[A_0 + \int_0^\infty \Phi(t) dt \right] q_{st} \quad (26)$$

and a steady aerodynamic force of the model is written as

$$f_{st_{model}} = [A_0 - HF^{-1}G] q_{st} \quad (27)$$

The following static aerodynamic force condition is added at the beginning of the consistency conditions of the Marcov parameters (17),

$$HF^{-1}G = - \int_0^\infty \Phi(t) dt \quad (28)$$

The last condition in Eq. (17),

$$HF^{2p-1}G = \Phi^{(2p-1)}(0+) \quad (29)$$

is deleted to maintain the number of conditions. The algorithm of model construction can be modified easily by shifting Marcov parameters and replacing H with HF^{-1} .

The characteristics of this approximate model are also interpreted in the frequency domain such that the frequency response of the model is consistent with the exact response at the point $k=0$, and the asymptotic series of the two systems are equal to the $(-2p+1)$ th order of jk .

This model is expected to give better accuracy in the low-frequency region. However, since the characteristic of the weighting pattern function of unsteady aerodynamics, i.e., that the memory does not fade away exponentially, affects the model, it is possible that system stability might be badly affected.

Example

In this section, a simple example is taken to illustrate the model construction method and properties of accuracy of the model. The flexible lifting surface considered here is a wind tunnel model of a cantilever wing, the planform of which is rectangular and has an aspect ratio equal to 6, as shown in Fig. 1.

Three flexible modes are chosen as follows.

Bending mode

$$Z_{a_1}(x, y) = 0.5(\cosh y^* - \cos y^*) - 0.367(\sinh y^* - \sin y^*)$$

$$y^* = 0.3125y$$

Torsion mode

$$Z_{a_2}(x, y) = -x \sin(\pi y/12)$$

Control mode

$$Z_{a_3}(x, y) = -(x - 0.2); \quad 0.2 \leq x \leq 1, \quad 3.6 \leq y \leq 6 \quad (30)$$

Aerodynamic data $A_2, A_1, A_0, \Phi(0), \dot{\Phi}(0+), \dots, \Phi^{(2p-1)}(0+)$ that are necessary for the model can be calculated by two possible ways. One way is to estimate the asymptotic series of frequency response from the aerodynamic matrices of high frequencies; the other is to estimate the Maclaurin series of time response produced by appropriately defined inputs (7). Since the major concern of frequency response of unsteady aerodynamics in aeroelasticity is in the low-frequency region, an adequate numerical program which yields results in the high-frequency region that are accurate enough to estimate the asymptotic series has not been developed. On the contrary, the time response calculation can be accomplished easily with a numerical simulation of the flowfield by an adequate method such as a vortex lattice method; and if the discretized length of timewise direction is sufficiently small,

Table 1 Aerodynamic data of the example

| | | | |
|-----------------------------|--------------|--------------|--------------|
| | -0.74286E+01 | -0.20842E+00 | 0.10160E+01 |
| A_2 | -0.20842E+00 | -0.22143E+01 | -0.49494E+00 |
| | 0.10160E+01 | -0.49494E+00 | -0.39502E+00 |
| | -0.55555E+01 | 0.16371E+02 | 0.63809E+01 |
| A_1 | -0.41962E+01 | -0.30736E+01 | -0.23197E+01 |
| | 0.18078E+00 | -0.25377E+01 | -0.19390E+01 |
| | -0.86901E+00 | 0.88658E+01 | 0.62557E+01 |
| A_0 | -0.69798E+00 | 0.70444E+01 | -0.55901E-01 |
| | 0.28893E-01 | -0.29097E+00 | -0.73215E+00 |
| | 0.65358E+00 | 0.87952E+00 | 0.40480E+00 |
| $\Phi(0)$ | 0.50293E+00 | 0.74862E+00 | 0.32532E+00 |
| | -0.21774E-01 | -0.29136E-01 | -0.13476E-01 |
| | -0.70003E+00 | -0.44508E+00 | -0.22520E+00 |
| $\dot{\Phi}(0)$ | -0.52393E+00 | -0.37229E+00 | -0.17429E+00 |
| | 0.23203E-01 | 0.14920E-01 | 0.75653E-02 |
| | 0.97379E+00 | 0.25165E+00 | 0.13034E+00 |
| $\ddot{\Phi}(0)$ | 0.71930E+00 | 0.21119E+00 | 0.99712E-01 |
| | -0.31955E-01 | -0.86842E-02 | -0.44426E-02 |
| | -0.14811E+01 | -0.83440E-01 | -0.28217E-01 |
| $\Phi^{(3)}(0)$ | -0.10893E+01 | -0.79793E-01 | -0.25275E-01 |
| | 0.48126E-01 | 0.33785E-02 | 0.10846E-02 |
| | -0.86900E+00 | -0.23712E+01 | -0.99294E+00 |
| $-\int_0^\infty \Phi(t) dt$ | -0.69798E+00 | -0.20505E+01 | -0.83180E+00 |
| | 0.28893E-01 | 0.78044E-01 | 0.32791E-01 |

time derivatives of the response can be estimated with accuracy. Since the time response necessary for the model construction is that of short time from the beginning of motion, the wake region to be considered is small. This property simplifies the vortex method. Therefore, aerodynamic data have been estimated from the time response by the vortex lattice method, which is briefly described in the Appendix. The accuracy of the method has been evaluated with an aerodynamic system in two-dimensional flow,¹⁵ where aerodynamic forces are analytically obtainable.

Aerodynamic data of the example are shown in Table 1. Construction of the models with and without a static condition is carried out by the method previously mentioned. In each case, two models that are different in degrees of approximation are obtained, i.e., $p=1$ and $p=2$. Since three modes are considered, orders of the augmented systems are third order and sixth order. The system triplet (F, G, H) of each model is listed in Table 2. Diagonalization has been carried out with similarity transformation in order to make the system characteristics clear. The triplet (F, G, H) of the diagonalized augmented system are defined as follows:

$$F = \text{diag}\{\lambda_1, \lambda_2, \dots, \lambda_N\}$$

$$G^T = [g_1, g_2, \dots, g_N], \quad H = [h_1, h_2, \dots, h_N] \quad (31)$$

where λ_i is a scalar and g_i, h_i are column vectors of m dimension.

The third-order model with a static condition shown in Table 2c has a pole in the right half of the s plane, i.e., it has an unstable mode. The consistency condition of steady aerodynamic forces generally introduces reduction in system damping. Furthermore in this case a lack of model order makes it unstable. Since an unstable model can not be adopted, the remaining three models will be discussed.

The accuracy of these models can be evaluated with frequency responses. As there are both three inputs and outputs nine elements of the aerodynamic matrix must be considered, but only typical elements are shown here due to space limitations. Frequency responses of the models and simple harmonic analysis are compared in Figs. 2-6.

Figure 2 is a Bode plot of bending-bending response, which means a generalized force of the bending mode caused by its motion. Responses of the three augmented state models and the nonmemory component of aerodynamic force, denoted by the "0th-order" model, are shown. In order to evaluate errors caused by finite dimensionalization by the models, responses derived by simple harmonic analysis are plotted, which are denoted "vortex method." They are calculated with the vortex lattice method by assuming simple harmonic motion and integrating wake vortices of sufficiently large length. Since the spacewise discretization with vortices in the calculation is equivalent to that of time response, which was adopted for the Marcov parameter calculation, only the approximation with finite state models is responsible for the resulting difference. Since the amplitude ratio varies widely in this frequency range, it is plotted in decibels. In the region of $k > 1$, the difference between the response of models, including the 0th order, and the simple harmonic results are remarkably reduced with the increase of frequency k . As shown in the figure, there is no noticeable difference in the high-frequency region. This characteristic is quite natural because of the conditions given for the model construction. Augmented state models are better than the 0th-order model in the low-frequency region. Among augmented state models, the sixth order models are better than the third-order model.

Figure 3 is a comparison of memory components through which accuracy properties of models can be directly observed. It shows responses of the augmented systems in each model and simple harmonic results that are obtained by extracting the nonmemory component from the previous "vortex method" results. The amplitude ratio is plotted on a linear scale in this and subsequent figures.

Figures 4-6 are Bode plots of other typical elements of the aerodynamic matrix. Since the accuracy of these models in the high-frequency region is unquestionable, in fact the error rapidly decreases in the region $k > 1$, accuracy properties in the low-frequency region are shown in the figures. The sixth-order models with and without a static condition have high accuracy, although the model with a static condition is slightly better than the model without a static condition in the region of $k \leq 0.1$. The third-order model also has reasonable ac-

Table 2a System triplet of the third-order model without a static condition

| $\text{Re}[\lambda_1]$ | $\text{Im}[\lambda_1]$ | λ_3 |
|------------------------|------------------------|-------------|
| -0.6602 | 0.1209 | -4.449 |
| $\text{Re}[g_1]$ | $\text{Im}[g_1]$ | g_3 |
| 0.3699 | 0.02773 | 0.08726 |
| 0.5895 | 0.3072 | -0.06439 |
| 0.2656 | 0.06922 | -0.01832 |
| $\text{Re}[h_1]$ | $\text{Im}[h_1]$ | h_3 |
| 0.7895 | 0 | 0.7963 |
| 0.5985 | -0.1333 | 0.6044 |
| -0.0264 | -0.000508 | -0.02603 |

Table 2c System triplet of the third-order model with a static condition

| λ_1 | λ_2 | λ_3 |
|-------------|-------------|-------------|
| -0.5269 | -0.7400 | 0.5842 |
| g_1 | g_2 | g_3 |
| -0.3904 | 0.3731 | 0.06905 |
| -1.014 | 0.4875 | -0.3338 |
| -0.3889 | 0.2616 | -0.1248 |
| h_1 | h_2 | h_3 |
| -0.7026 | 0.8729 | 0.7758 |
| -0.7112 | 0.4870 | 0.6305 |
| 0.02277 | -0.02982 | -0.02548 |

Table 2b System triplet of the sixth-order model without a static condition

| λ_1 | $\text{Re}[\lambda_2]$ | $\text{Im}[\lambda_2]$ | λ_4 | λ_5 | λ_6 |
|-------------|------------------------|------------------------|-------------|-------------|-------------|
| -0.3110 | -0.9559 | 0.02395 | -3.003 | -2.043 | -4.540 |
| g_1 | $\text{Re}[g_2]$ | $\text{Im}[g_2]$ | g_4 | g_5 | g_6 |
| 0.1714 | 0.2679 | 0.5443 | -0.09355 | 0.03492 | -0.01647 |
| 0.8273 | 0.1711 | 1.239 | 0.03520 | 0.00064 | 0.006035 |
| 0.2922 | 0.1246 | 0.01848 | 0.001402 | -0.02052 | 0.000235 |
| h_1 | $\text{Re}[h_2]$ | $\text{Im}[h_2]$ | h_4 | h_5 | h_6 |
| 0.7565 | 0.8086 | 0 | -0.8061 | 0.8190 | 0.8076 |
| 0.6535 | 0.5877 | -0.00959 | -0.5912 | 0.5732 | 0.5891 |
| -0.02488 | -0.02725 | -0.000014 | 0.02577 | -0.02695 | -0.02595 |

Table 2d System triplet of the sixth-order model with a static condition

| | | | | | |
|-------------|-------------|-------------|-------------|------------------------|------------------------|
| λ_1 | λ_2 | λ_3 | λ_4 | $\text{Re}[\lambda_5]$ | $\text{Im}[\lambda_5]$ |
| -0.8737 | -0.2407 | -0.5979 | -1.718 | -2.659 | 0.5007 |
| g_1 | g_2 | g_3 | g_4 | $\text{Re}[g_5]$ | $\text{Im}[g_5]$ |
| -0.5300 | 0.08998 | 0.03260 | -0.07842 | 0.04757 | -0.01887 |
| -0.4845 | 0.5795 | 0.1077 | -0.02913 | -0.02045 | 0.01663 |
| -0.2970 | 0.2267 | 0.01431 | 0.01014 | -0.003759 | 0.000192 |
| h_1 | h_2 | h_3 | h_4 | $\text{Re}[h_5]$ | $\text{Im}[h_5]$ |
| -0.8048 | 0.7559 | 0.5904 | -0.7636 | 0.8397 | 0. |
| -0.5929 | 0.6542 | 0.8069 | -0.6452 | 0.5408 | 0.04046 |
| 0.02711 | -0.02479 | -0.01862 | 0.0252 | -0.02747 | 0.000503 |

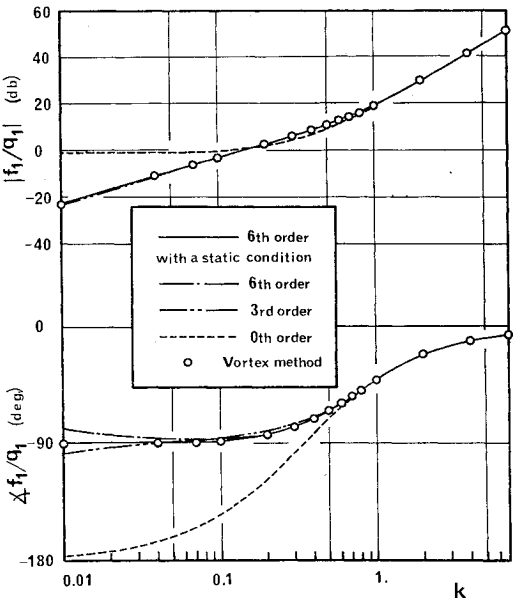


Fig. 2 Bode plot of generalized force of bending mode due to bending mode motion.

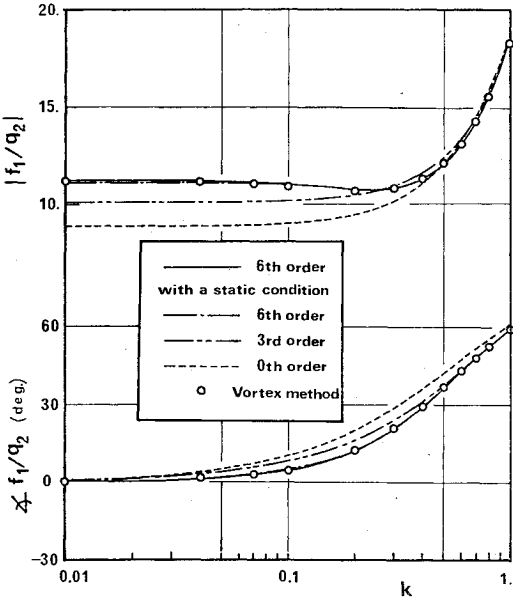


Fig. 4 Bode plot of generalized force of bending mode due to torsion mode motion.

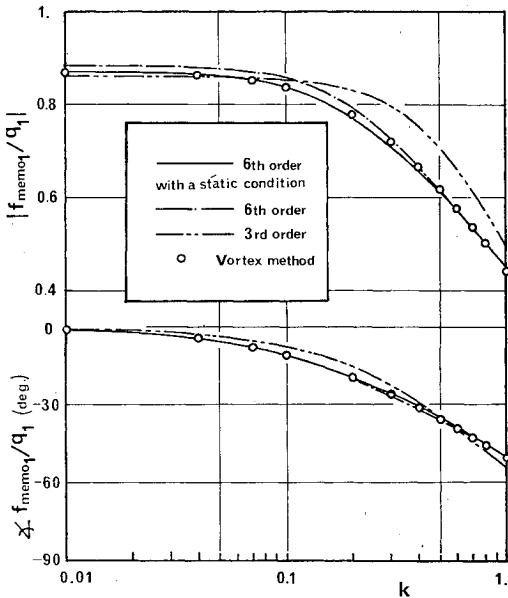


Fig. 3 Bode plot of memory component in generalized force of bending mode due to bending mode motion.

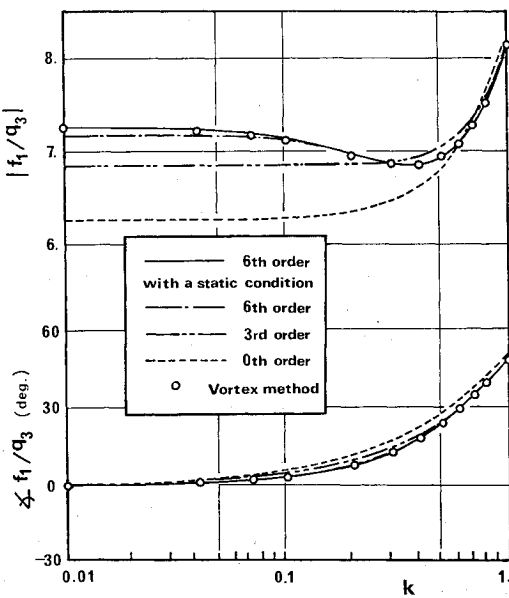


Fig. 5 Bode plot of generalized force of bending mode due to control mode motion.

curacy. The 0th-order model, the nonmemory component of aerodynamic force, gives poor accuracy in the low-frequency region in phase plots of some matrix elements. The augmented state model proposed here has greater accuracy in the high-frequency region as its order increases.

This example, however, shows that approximation improvement by increasing the order has sufficient effects on the accuracy in the low-frequency region. The ninth-order model is also stable and has better accuracy than the sixth-order models, although the result is not shown

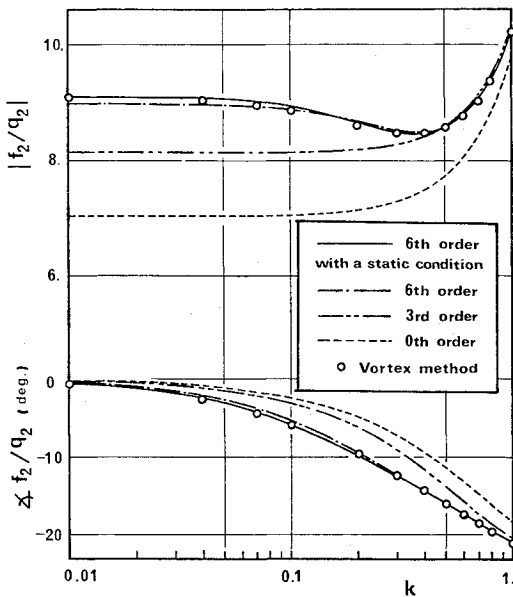


Fig. 6 Bode plot of generalized force of torsion mode due to torsion mode motion.

in this paper. It can be considered that an increase of degree in the approximation does not diminish system stability. It is a characteristic of this model that the error of time response is highly weighted in the vicinity of $t=0$; in other words, the error of frequency response is highly weighted in the high-frequency region.

Concluding Remarks

The paper has proposed a method for constructing a finite state model that simulates an unsteady aerodynamic system of a lifting surface in incompressible flow. Generalized aerodynamic forces produced by an arbitrary motion are expressed explicitly by generalized coordinates in the time domain. The formulation introduces the separation of aerodynamic forces into two components, i.e., the non-memory and memory components. In order to formulate a state equation of the total aeroelastic system, only the latter component must be approximately made to be of finite dimension by using an augmented system. The augmented system is proposed to be generated from Markov parameters of the aerodynamic system. In the frequency domain, the asymptotic series of the model response is consistent with that of the aerodynamic system of some order.

The numerical example shows good properties in approximation and system stability. The stability of the model is easily guaranteed, because 1) the augmented system is constructed only from the memory component of unsteady aerodynamics, the stability of which is guaranteed by nature, and 2) the model error is highly weighted in the high-frequency region. Through the construction of the model, the designer has to arrange only one parameter, which determines the degree of approximation. Since there is no need for weighting parameters and data points of frequency, which are necessary in ordinary least square methods, the model can be obtained directly. Frequency response errors caused by finite dimensionalization are evaluated by the numerical example. It shows that accuracy of the models is good not only in the high-frequency region but also in the low-frequency region. This means that the aerodynamic system involves a great deal of information in the high-frequency region, and that the model constructed from Markov parameters can be useful for analysis and synthesis of aeroelastic control systems.

Appendix

A vortex method which has been adopted for the numerical calculation of the unsteady aerodynamic data is briefly shown. This Appendix is limited to the calculation for the

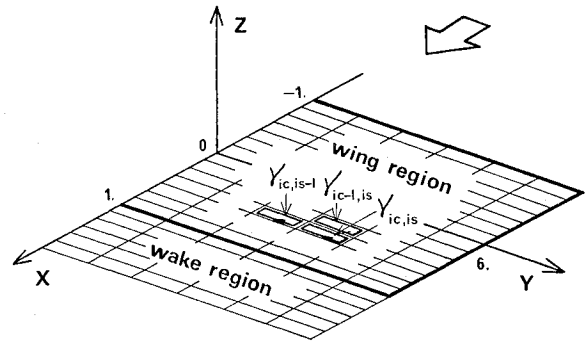


Fig. A1 Vortex lattice sheet on the wing and wake.

example in the text. More detailed discussions have been given in Refs. 15 and 16.

Figure A1 shows a vortex sheet that expands on a lifting surface and its wake. It is assumed, for simplicity, that each element has the same shape. The discretized time interval Δt is defined to be equal to the chordwise length of each element Δx , i.e., Δt is chosen to be the length of time that the flow takes to move Δx . All quantities are dimensionless. As shown in Fig. A1, at a time $\ell\Delta t$ after the motion begins, the wake region is expanded downstream to the length $(\ell-1)\Delta x$, where an integer ℓ denotes the sequence of discrete time steps. Closed vortices of rectangular form which encircle each element are distributed on the wing and wake. The intensity of each vortex is defined as $\gamma_{ic,is}$, where the double subscript ic,is denotes chordwise and spanwise order, respectively. Each vortex generates a potential discontinuity $\Delta\phi(x,y,t)$, which has a value equal to $\gamma_{ic,is}$ only in its own element and is constant over the element. The pressure difference between the upper and lower surfaces of the wing $\Delta C_p(x,y,t)$ is expressed by a substantial derivative of the potential discontinuity, namely,

$$\Delta C_p(x,y,t) = -2\{\partial\Delta\phi(x,y,t)/\partial x + \partial\Delta\phi(x,y,t)/\partial t\} \quad (A1)$$

The discretized pressure distribution can be defined as,

$$\Delta C_{p_{ic,is}}((\ell-1/2)\Delta t) = -2\{\gamma_{ic,is}(\ell\Delta t) - \gamma_{ic-1,is}((\ell-1)\Delta t)\}/\Delta x \quad (A2)$$

Since the time derivative is introduced from the difference between the ℓ th and $(\ell-1)$ th time values and the x derivative is introduced from the difference between the ic th and the $(ic-1)$ th element values, the pressure distribution defined by Eq. (A2) can be considered to represent the pressure value of leading edge of the ic th element at the time $(\ell-1/2)\Delta t$. Since there is no pressure difference in the wake region, $\gamma_{ic,is}(\ell\Delta t)$ is equal to $\gamma_{ic-1,is}((\ell-1)\Delta t)$. This means that the intensity of the vortex in the wake region is preserved and only its location is changed downstream with the flow.

The discrete-time response of vortices on the wing is determined by the boundary conditions of downwash distribution. When the response due to the j th generalized coordinate input is under consideration, the downwash distribution is given from Eqs. (6) and (7)

$$w_{ic,is}(\ell\Delta t) = Z_{a_j}(x,y)(\ell\Delta t) + \partial Z_{a_j}(x,y)/\partial x(\ell\Delta t)^2/2 \quad (A3)$$

where (x,y) is a collocation point on the wing region.

The downwash distribution produced by a rectangular form vortex is analytically obtainable with the Biot-Savart law. Because of linearity, the downwash at a certain point on the xy plane is obtained by superposing contributions of all vortices. If the boundary condition is considered to be satisfied at the geometric center of each element, it is expressed with matrices and vectors as follows:

$$A_{\text{wing}}\gamma_{\text{wing}}(\ell\Delta t) + A_{\text{wake}}(\ell\Delta t)\gamma_{\text{wake}}(\ell\Delta t) = w(\ell\Delta t) \quad (A4)$$

where vectors γ_{wing} and γ_{wake} consist of all vortices $\gamma_{ic, is}$ on the wing and on the wake, respectively, and a vector w consists of all downwash on the wing $w_{ic, is}$. A_{wing} and A_{wake} are appropriately defined influence-coefficient matrices. The constant square matrix A_{wing} is nonsingular. Since the vortices on the wake γ_{wake} at the time $\ell\Delta t$ are directly expressed by vortices at the time $(\ell-1)\Delta t$, the boundary condition (A4) is more suitably rewritten as follows:

$$\gamma_{\text{wing}}(\ell\Delta t) = A_{\text{wing}}^{-1} \{ w(\ell\Delta t) - A_{\text{wake}}(\ell\Delta t) \gamma_{\text{wake}}(\ell\Delta t) \} \quad (\text{A5})$$

From the above equation, the responses of vortices on the wing are sequentially obtainable, and the pressure distribution can be calculated from Eq. (A2). Summing up the pressure distribution with appropriate weightings corresponding to each mode shape $Z_{aj}(x, y)$, the i th generalized force response of discrete time steps $\Phi_{ij}^o((\ell-1/2)\Delta t)$ can be obtained.

The response function of generalized force, $\Phi_{ij}^o(t)$ and its higher order derivatives at $t=0$, i.e., $\Phi_{ij}^o(0)$, $\Phi_{ij}^o(0+)$, $\Phi_{ij}^o(0+)$, ..., $\Phi_{ij}^o(2p+2)(0+)$ can be estimated from the discrete-time response by using ordinary numerical differentiation.

Since it is necessary in the numerical computation to store the values of vortices on the wake and to calculate their effects on the wing downwash, this method can be considered to be more suitable for the short time response from the beginning of motion.

Static Aerodynamic Force

Steady-state pressure distribution can be calculated by considering that the vortices of each element are time invariant. The wake region is infinitely extended downstream. However, since intensities of the vortices on the wake are constant in the stream direction, they can be summed to be horseshoe vortices which originate from the trailing edge elements. The boundary condition for the steady vortices on the wing $\gamma_{\text{wing, st}}$ is written as

$$A_{\text{st}} \gamma_{\text{wing, st}} = w_{\text{st}} \quad (\text{A6})$$

where vectors $\gamma_{\text{wing, st}}$ and w_{st} consist of vortices $\gamma_{ic, is}$ and downwash distribution $w_{ic, is}$, respectively. The influence matrix A_{st} , which can be analytically defined, is nonsingular. When the response of unit input of the j th generalized coordinate is considered, the downwash distribution is defined as

$$w_{ic, is} = \partial Z_{aj}(x, y) / \partial x \quad (\text{A7})$$

where the coordinate (x, y) is the geometric center of the (ic, is) element. From Eq. (A6), vortex distributions can be calculated. The pressure distribution and the generalized force can be obtained in the same way as the time response calculation.

Acknowledgments

The authors would like to express their appreciation to Dr. T. Ichikawa, Dr. M. Komoda, and Dr. N. Kawahata of the National Aerospace Laboratory for their helpful suggestions and criticisms.

References

- ¹Edwards, J. W., Breakwell, J. V., and Bryson, A. E., "Active Flutter Control Using Generalized Unsteady Aerodynamic Theory," *Journal of Guidance and Control*, Vol. 1, Jan.-Feb. 1978, pp. 32-40.
- ²Abel, I., Perry, B., and Murrow, H. N., "Two Synthesis Techniques Applied to Flutter Suppression on a Flight Research Wing," *Journal of Guidance and Control*, Vol. 1, Sept.-Oct. 1978, pp. 340-346.
- ³Newsom, J. R., "Control Law Synthesis for Active Flutter Suppression Using Optimal Control Theory," *Journal of Guidance and Control*, Vol. 2, Sept.-Oct. 1979, pp. 388-394.
- ⁴Mahesh, J. K., Stone, C. R., Garrard, W. L., and Dunn, H. J., "Control Law Synthesis for Flutter Suppression Using Linear Quadratic Gaussian Theory," *Journal of Guidance and Control*, Vol. 4, July-Aug. 1981, pp. 415-422.
- ⁵Vepa, R., "Finite State Modeling of Aeroelastic Systems," NASA CR-2779, 1977.
- ⁶Edwards, J. W., "Application of Laplace Transform Methods to Airfoil Motion and Stability Calculations," AIAA Paper 79-0772, April 1979.
- ⁷Albano, E. and Rodden, W. P., "A Doublet-Lattice Method for Calculating Lift Distributions on Oscillating Surfaces in Subsonic Flows," *AIAA Journal*, Vol. 7, Feb. 1969, pp. 279-285.
- ⁸Rowe, W. S., Winther, B. A., and Redman, M. C., "Prediction of Unsteady Aerodynamic Loadings Caused by Trailing Edge Control Surface Motions in Subsonic Compressible Flow—Analysis and Results," NASA CR-2003, June 1972.
- ⁹Li, J. M., "Synthesis of Aerodynamic Transfer Functions for Elastic Flight Vehicles," *Journal of Aircraft*, Vol. 15, Nov. 1978, pp. 777-785.
- ¹⁰Schwanz, R. C., "A Criterion to Judge the Accuracy of Frequency Domain Approximating Functions," AIAA Paper 80-0767, 1980.
- ¹¹Roger, K. L., "Airplane Math Modeling Methods for Active Control Design," AGARD CP-228, Aug. 1977, pp. 4.1-4.11.
- ¹²Zadeh, L. A. and Desoer, C. A., *Linear System Theory: The State Space Approach*, McGraw-Hill, New York, 1963.
- ¹³Ho, B. L. and Kalman, R. E., "Effective Construction of Linear State-Variable Models from Input/Output Functions," *Regelungstechnik*, Heft 12, 1966, pp. 545-548.
- ¹⁴Tether, A. J., "Construction of Minimal Linear State-Variable from Finite Input-Output Data," *IEEE Transactions on Automatic Control*, Vol. AC-15, No. 4, 1970, pp. 427-436.
- ¹⁵Miyazawa, Y., "Time Response Approach to Numerical Computation of Asymptotic Series in Unsteady Aerodynamics for a Lifting Surface in Incompressible Flow," Technical Report of National Aerospace Laboratory TR-721T, 1982.
- ¹⁶Miyazawa, Y., "Active Controls for Aeroelastic Systems," (in Japanese) Ph.D. Dissertation, University of Tokyo, 1981.